Bulletin of the Seismological Society of America, Vol. 99, No. 2B, pp. 1423–1428, May 2009, doi: 10.1785/0120080154

Short Note

Waves in Linear Elastic Media with Microrotations, Part 2: Isotropic Reduced Cosserat Model

by E. F. Grekova,* M. A. Kulesh, and G. C. Herman†

Abstract We consider wave propagation in soils and rocks modeled as an isotropic linear elastic reduced Cosserat continuum to take into account the proper rotational dynamics of heterogeneities contained in media. In such a medium, translations and rotations are kinematically independent, the stress tensor is nonsymmetric, and the couple stresses are zero. We consider plane wave propagation, construct the Green's function for the harmonic point source in the 3D unbounded medium, and study the Rayleigh-type wave. The compression wave for the isotropic case is the same as in the classical medium. The shear wave is coupled with rotation and differs both from the classical case and from the case of the full Cosserat continuum. There are forbidden bands of frequencies where some waves do not propagate, localization phenomena are possible, and strongly dispersive behavior is observed near these bands. For the Rayleigh wave, there is also a cutoff wavenumber for one of the dispersion branches.

Introduction

Rocks are continua of complex structure that are modeled in various ways in the literature. Apart from models taking into account the details of the microstructure, there are models based on effective media (Hudson and Knopoff, 1989). These anisotropic models replace the actual heterogeneous medium via some averaging procedure by an anisotropic, but homogeneous, medium. In this way, complexity and spatial heterogeneity are replaced by anisotropy (of a homogeneous effective medium). By the very nature of the averaging process, these methods do not account for frequency-dependent effects.

One of the possible ways to take into account microstructural degrees of freedom is to consider the rotational dynamics of heterogeneities that are contained in rocks and soils; for the importance of rotational dynamics in seismology see references in Kulesh (2009). Many researchers use the full Cosserat continuum model to model soils and granular materials, for example, Vardoulakis (1989) and Suiker *et al.* (2001). The first time, the 3D medium consisting of point-bodies possessing rotational degrees of freedom was suggested by Cosserat and Cosserat (1909). The complete constitutive theory of the Cosserat continuum was suggested by Kafadar and Eringen (1971). Basic equations and wave problems for the Cosserat elasticity also can be found in Nowacki (1986) or in Eringen (1998).

This may be done in the frame of the model of an effective homogeneous elastic reduced Cosserat continuum. Schwartz *et al.* (1984) suggested this theory for the first time for the description of granular materials in its isotropic variant.

In this model, point bodies of the continuum can rotate and move, and their rotations and translations are kinematically independent. The medium reacts to the rotation of a point body relative to the background continuum, but there is no rotational spring trying to reduce the relative turn of point bodies. This means that the stress tensor is asymmetric, but the couple stress tensor is zero (contrary to the complete Cosserat continuum).

The reduced Cosserat continuum will be more appropriate for the description of those media where there is no elastic reaction counteractive to the relative rotation of neighboring heterogeneities. The full Cosserat medium, discussed in Kulesh (2009), will better describe those media where such a reaction is present. Probably, only an experiment can answer the question, Which model is more suitable for a concrete medium? We present the results on wave propagation in both media, which can be used as a theoretical base to suggest an appropriate experiment.

In this paper, we shall consider wave propagation in the isotropic reduced Cosserat continuum: plane waves, waves

*Current address: Departmento Electrónica y Electromagnetismo, University of Seville, Avenida Reina Mercedes s/n, 41012, Seville, Spain

†Deceased, 24 August 2006.

caused by dynamical point sources for the unbounded 3D medium, and the Rayleigh-type wave. The Green's function for a classical elastic half-space was first published in Okada (1985). The Green's functions are necessary both for the analysis of the displacements produced by earthquakes as well as for the deformations arising from fluid-driven crack sources. The Green's functions presented in this article are obtained for an unbounded 3D reduced Cosserat continuum; therefore, they may be used for the calculation of the same fields but far enough from the surface or before the wave is reflected from it. We cannot obtain these solutions as a particular case of the corresponding solutions for the full Cosserat continuum because the order of the partial differential equations is different; therefore, we investigate the case of the reduced Cosserat continuum separately.

Basic Equations

Let $\tilde{e}$ be the unit tensor, $\tilde{\sigma}$ be the stress tensor, U be the elastic energy, $\mathbf{u}$ be the vector of an infinitesimal displacement, $\boldsymbol{\theta}$ be the vector of an infinitesimal rotation of the point body, and ρ be the density of the medium. For simplicity, we consider the inertia tensor to be spherical and equal to $j\tilde{e}$, where j is the mass density of the inertia moment. Let us denote by $\mathbf{X}$ and $\mathbf{Y}$ the external volume force and torque, respectively.

The elastic energy in the complete linear elastic Cosserat continuum depends on the following deformation tensors (Eringen, 1998): $(\operatorname{grad}\mathbf{u})^S$, $(\operatorname{grad}\mathbf{u}+\boldsymbol{\theta}\times\tilde{e})^A$, and $\operatorname{grad}\boldsymbol{\theta}$. In the reduced Cosserat continuum, according to our assumption, there is no dependence on $\operatorname{grad}\boldsymbol{\theta}$, that is, the elastic constants β, γ, and ε used in Kulesh (2009) are zero. Therefore, U has to be a quadratic form of $\operatorname{grad}\mathbf{u}+\boldsymbol{\theta}\times\tilde{e}$. For the isotropic case, we have only three elastic constants: Lamé coefficients λ, μ, and one (new) rotational constant α, an elastic constant characterizing the resistance of the medium to the rotation of a particle. The equations of motion are the particular case ($\beta=\gamma=\varepsilon=0$) of those in Kulesh (2009):

$$\begin{aligned}
\tilde{\sigma} &= 2\mu\tilde{\gamma}^{(S)} + 2\alpha\tilde{\gamma}^{(A)} + \lambda I_1(\tilde{\gamma})\tilde{e},\\
\tilde{\gamma} &= \operatorname{grad}\mathbf{u} + \boldsymbol{\theta}\times\tilde{e},\\
(\lambda+2\mu)\operatorname{grad}\operatorname{div}\mathbf{u} &- (\mu+\alpha)\operatorname{rot}\operatorname{rot}\mathbf{u} + 2\alpha\operatorname{rot}\boldsymbol{\theta} + \mathbf{X}\\
&= \rho\ddot{\mathbf{u}},\\
2\alpha\operatorname{rot}\mathbf{u} &- 4\alpha\boldsymbol{\theta} + \mathbf{Y} = j\ddot{\boldsymbol{\theta}}.
\end{aligned} \tag{1}$$

However, the solutions cannot be obtained directly from those for the full Cosserat continuum setting $\beta=\gamma=\varepsilon=0$ because the order of the partial differential equations is changed.

The equations of classical elasticity for $\mathbf{u}$ follow from equation (1) in two limiting cases: (1) $\alpha=0$ (the medium does not resist at all to the rotation of particles, the equation for $\boldsymbol{\theta}$ is separated, and rotation waves do not propagate) and (2) $\alpha\to\infty$ (Cosserat pseudocontinuum, the particles are rigidly embedded into the medium, $\boldsymbol{\theta}=1/2\operatorname{rot}\mathbf{u}$).

In the static case ($\ddot{\boldsymbol{\theta}}=0$) and in absence of external torque loads ($\mathbf{Y}=0$) we have again the latter case. However, the wave behavior of the medium is more complex than in the classical case. Equation (1) gives us a relation between the rotational and translational displacements: $\boldsymbol{\theta}=1/2\operatorname{rot}\mathbf{u}+(\mathbf{Y}-j\ddot{\boldsymbol{\theta}})/(4\alpha)$, which differs from the analogous relation for the Cosserat pseudocontinuum by the last term.

Dispersion Curves for the 3D Case

Let us introduce the following magnitudes: $C_l^2=(\lambda+2\mu)/\rho$, $C_s^2=\mu/\rho$, $C_{s\alpha}^2=(\mu+\alpha)/\rho$, $\omega_0^2=4\alpha/j$, and $\omega_1^2=\omega_0^2/(1+\alpha/\mu)$.

Using Sandru representation via potentials $\boldsymbol{\Phi}_1$ and $\boldsymbol{\Phi}_2$ (Eringen, 1998), we separate equations (1) into the form:

$$\begin{aligned}
\Box_1(\Box_2\Box_3+4\alpha^2\triangle)\boldsymbol{\Phi}_1 &= -\rho\mathbf{X},\\
\Box_3(\Box_2\Box_3+4\alpha^2\triangle)\boldsymbol{\Phi}_2 &= -\rho\mathbf{Y},
\end{aligned} \tag{2}$$

where $\Box_1=(\lambda+2\mu)(\triangle-C_l^{-2}\partial_t^2)$, $\Box_2=(\mu+\alpha)\times(\triangle-C_{s\alpha}^{-2}\partial_t^2)$, and $\Box_3=-4\alpha(1+\omega_0^{-2}\partial_t^2)$.

The translational and angular displacements can be found via these potentials in the following way:

$$\begin{aligned}
\mathbf{u} &= \Box_1\Box_3\boldsymbol{\Phi}_1 - [(\lambda+\mu-\alpha)\Box_3-4\alpha^2]\operatorname{grad}\operatorname{div}\boldsymbol{\Phi}_1\\
&\quad - 2\alpha\Box_3\operatorname{rot}\boldsymbol{\Phi}_2,\\
\boldsymbol{\theta} &= \Box_2\Box_3\boldsymbol{\Phi}_2 + 4\alpha^2\operatorname{grad}\operatorname{div}\boldsymbol{\Phi}_2 - 2\alpha\Box_1\operatorname{rot}\boldsymbol{\Phi}_1.
\end{aligned} \tag{3}$$

In this section, we consider zero external loads $\mathbf{X}$ and $\mathbf{Y}$ and look for the plane-wave solution of (1): $\boldsymbol{\Phi}_1=\boldsymbol{\Phi}_{1(0)}e^{i(\mathbf{k}\cdot\mathbf{r}-\omega t)}$ and $\boldsymbol{\Phi}_2=\boldsymbol{\Phi}_{2(0)}e^{i(\mathbf{k}\cdot\mathbf{r}-\omega t)}$, where $\mathbf{k}$ is the wave vector, $k=|\mathbf{k}|$, ω is the angular frequency, $\boldsymbol{\Phi}_{1(0)}$ and $\boldsymbol{\Phi}_{2(0)}$ are the amplitudes of the potentials $\boldsymbol{\Phi}_1$, $\boldsymbol{\Phi}_2$, and $\mathbf{r}$ is the radius vector.

Substituting this representation in (2) with $\mathbf{X}$, $\mathbf{Y}$ both zero, we obtain the dispersion relations. The compression wave does not change its character in comparison to the classical continuum with Lamé constants λ and μ, and its velocity equals C_l. The shear wave, on the contrary, changes essentially in that range of frequencies where the rotation of particles with respect to the bulk is important. The shear wave is coupled with rotations, and as a consequence, the shear dispersion curve doubles. The shear dispersion relation is

$$k_S^2=\frac{\omega^2}{C_s^2}\,\frac{1-\omega^2/\omega_0^2}{1-\omega^2/\omega_1^2}=\frac{\omega^2}{C_s^2}f^2(\omega). \tag{4}$$

These dispersion curves are shown in Figure 1. At low and high frequencies, the medium behaves as a classical elastic continuum with compression-wave velocity C_l and shear-wave velocities C_s and $C_{s\alpha}$, respectively. There may appear one important difference: for $\alpha>\lambda+\mu$ the shear wave, though almost not dispersive at high frequencies, is faster

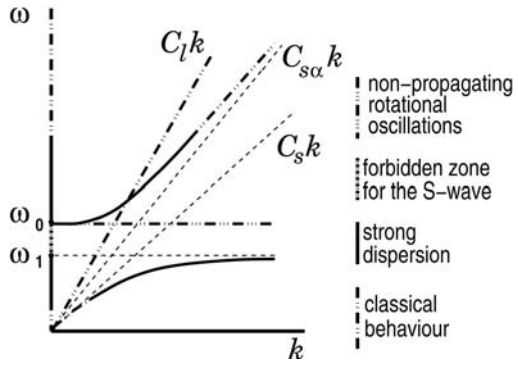

Figure 1. 3D dispersion curves. The *P* wave is not affected; the *S* wave is strongly frequency dependent and has a forbidden zone for $\omega_1 < \omega < \omega_0$, where the wave decays exponentially with depth.

than the compression wave (e.g., a classical medium with such [positive] elastic constants does not exist). At frequencies close to critical frequencies, ω_0 and ω_1, there is a strong dispersion and localization phenomenon. In the forbidden zone ($\omega_1 < \omega < \omega_0$) the shear plane waves do not propagate. The horizontal line $\omega = \omega_0$ on the figure corresponds to the free nonpropagating rotational oscillations of point bodies. The calculation of the eigenvectors for the plane-wave problem shows that the shear-rotation wave changes its character: it is not purely transversal, and the phase also changes. The expressions for displacements are

$$\begin{aligned}\mathbf{u} = {} & e^{i(\mathbf{k}_s\cdot\mathbf{r}-\omega t)}\{(\lambda+2\mu)(1-\omega^2/\omega_0^2)(k_s^2-\omega^2/C_l^2)\mathbf{a}_1 \\ & -[(\lambda+\mu-\alpha)(1-\omega^2/\omega_0^2)+\alpha]\mathbf{k}_s\mathbf{k}_s\cdot\mathbf{a}_1 \\ & + i2\alpha(1-\omega^2/\omega_0^2)\mathbf{k}_s\times\mathbf{a}_2\} \\ & + e^{i(\mathbf{k}_1\cdot\mathbf{r}-\omega t)}4\alpha\{-[(\lambda+\mu-\alpha)(1-\omega^2/\omega_0^2) \\ & + \alpha]\mathbf{k}_1\mathbf{k}_1\cdot\mathbf{A}_1\},\end{aligned} \tag{5}$$

$$\begin{aligned}\boldsymbol{\theta} = {} & e^{i(\mathbf{k}_s\cdot\mathbf{r}-\omega t)}2\alpha[2(\mu+\alpha)(1-\omega^2/\omega_0^2)(k_s^2-\omega^2/C_{s\alpha}^2)\mathbf{a}_1 \\ & - 2\alpha\mathbf{k}_s\mathbf{k}_s\cdot\mathbf{a}_2 + (\lambda+2\mu)(k_s^2-\omega^2/C_l^2)\mathbf{k}_s\times\mathbf{a}_1] \\ & + e^{i\omega_0 t}\,\mathrm{grad}\,\mathrm{div}\,\mathbf{A}_2(\mathbf{r}),\end{aligned} \tag{6}$$

where $\mathbf{a}_1$, $\mathbf{a}_2$, and $\mathbf{A}_1$ are arbitrary constant vectors and $\mathbf{A}_2$ is an arbitrary vectorial function of $\mathbf{r}$.

Green's Functions

Now consider the reaction of the system to the dynamic point source. This could be useful, for instance, to understand the character of waves, caused by the earthquake, before reflection from the surface. This is also a necessary step to obtain the solution for any type of sources distributed in space and time. Consider $\rho\mathbf{X} = \mathbf{X}_0\delta(\mathbf{r})e^{i\omega t}$ and $\rho\mathbf{Y} = \mathbf{Y}_0\delta(\mathbf{r})e^{i\omega t}$. Using the inverse Fourier transform, and using the fact

$$\int_{-\infty}^{+\infty}(k^2-k_1^2)^{-1}e^{-i\mathbf{k}\cdot\mathbf{r}}\,dk_x\,dk_y\,dk_z = 2\pi^2 e^{ik_1 r}/r, \tag{7}$$

we obtain the solution for the potentials:

$$\begin{aligned}\boldsymbol{\Phi}_1 &= \mathbf{x}_0 e^{i\omega t}(e^{-i\omega r/C_l} - e^{-i\omega f(\omega) r/C_s})/r, \\ \boldsymbol{\Phi}_2 &= \mathbf{y}_0 e^{i\omega t}e^{-i\omega f(\omega) r/C_s}/r,\end{aligned} \tag{8}$$

where

$$\begin{aligned}f(\omega) &= -i\sqrt{(1-\omega^2/\omega_0^2)/|1-\omega^2/\omega_1^2|}, \\ &\quad \text{if } \omega_1 < \omega < \omega_0; \\ f(\omega) &= \sqrt{(1-\omega^2/\omega_0^2)/(1-\omega^2/\omega_1^2)}, \\ &\quad \text{if } \omega > \omega_0 \quad \text{or} \quad \omega < \omega_1; \\ \mathbf{x}_0 &= -\mathbf{X}_0/\{16\pi\alpha\mu(\lambda+2\mu)(1-\omega^2/\omega_1^2)[\omega^2/C_l^2 \\ &\quad - \omega^2 f^2(\omega)/C_s^2]\}, \\ \mathbf{y}_0 &= \mathbf{Y}_0/[64\pi\alpha^2\mu(1-\omega^2/\omega_0^2)(1-\omega^2/\omega_1^2)].\end{aligned} \tag{9}$$

The expressions for $\mathbf{u}$ and $\boldsymbol{\theta}$ can be obtained from $\boldsymbol{\Phi}_1$ and $\boldsymbol{\Phi}_2$ using (3):

$$\begin{aligned}\mathbf{u} = {} & \frac{\mathbf{Y}_0 e^{i\omega t}}{8\pi\alpha\mu}\left(1-\frac{\omega^2}{\omega_1^2}\right)^{-1}\frac{\tilde{e}\times\hat{\mathbf{r}}}{r^2}\left(1+i\frac{\omega f(\omega)}{C_s}r\right)e^{-i\frac{\omega f(\omega)}{C_s}r} - \frac{\mathbf{X}_0 e^{i\omega t}}{4\pi\mu(\lambda+2\mu)}\left(\frac{\omega^2}{C_l^2}-\frac{\omega^2 f^2(\omega)}{C_s^2}\right)^{-1}\left(1-\frac{\omega^2}{\omega_1^2}\right)^{-1}\cdot\left(-e^{-i\frac{\omega}{C_l}r}\left[\left(\lambda+\mu\right.\right.\right. \\ & \left.\left.\left.-\alpha\right)\left(1-\frac{\omega^2}{\omega_0^2}\right)+\alpha\right]\left[\frac{1}{r}\frac{\omega^2}{C_l^2}\hat{\mathbf{r}}\,\hat{\mathbf{r}}+\left(1+i\frac{\omega}{C_l}r\right)\frac{\tilde{e}-3\hat{\mathbf{r}}\,\hat{\mathbf{r}}}{r^3}\right]+e^{-i\frac{\omega f(\omega)}{C_s}r}\left\{\frac{1}{r}\tilde{e}\left(1-\frac{\omega^2}{\omega_0^2}\right)(\lambda+2\mu)\left(\frac{\omega^2}{C_l^2}-\frac{\omega^2 f^2(\omega)}{C_s^2}\right)\right. \\ & \left.+\left[(\lambda+\mu-\alpha)\left(1-\frac{\omega^2}{\omega_0^2}\right)+\alpha\right]\left[\frac{1}{r}\frac{\omega^2 f^2(\omega)}{C_s^2}\hat{\mathbf{r}}\,\hat{\mathbf{r}}+\left(1+i\frac{\omega f(\omega)}{C_s}r\right)\frac{\tilde{e}-3\hat{\mathbf{r}}\,\hat{\mathbf{r}}}{r^3}\right]\right\}\Bigg),\end{aligned} \tag{10}$$

$$\begin{aligned}\boldsymbol{\theta} = {} & e^{i(\omega t-\frac{\omega f(\omega)}{C_s}r)}\left(1-\frac{\omega^2}{\omega_1^2}\right)^{-1}\left\{-\frac{\mathbf{X}_0}{8\pi\mu}\frac{\tilde{e}\times\hat{\mathbf{r}}}{r^2}\left(1+i\frac{\omega f(\omega)}{C_s}r\right)-\frac{\mathbf{Y}_0}{16\pi\alpha^2\mu}\left(1-\frac{\omega^2}{\omega_0^2}\right)^{-1}\cdot\left[\frac{1}{r}\tilde{e}\left(1-\frac{\omega^2}{\omega_0^2}\right)\left(\frac{\omega^2}{C_{s\alpha}^2}-\frac{\omega^2 f^2(\omega)}{C_s^2}\right)(\mu+\alpha)\right.\right. \\ & \left.\left.+\frac{1}{r}\hat{\mathbf{r}}\,\hat{\mathbf{r}}\frac{\omega^2 f^2(\omega)}{C_s^2}\alpha+\frac{1}{r^3}\left(1+i\frac{\omega f(\omega)}{C_s}r\right)(\tilde{e}-3\hat{\mathbf{r}}\,\hat{\mathbf{r}})\alpha\right]\right\},\end{aligned}$$

where $\hat{\mathbf{r}} = \mathbf{r}/|r|$.

The solution for $\mathbf{u}$ at $\omega \ll \omega_1$ and $\mathbf{Y}_0 = 0$ gives the Green's function of classical elasticity (Miklowitz, 1978) for a medium with phase velocities C_l (compression wave) and C_s (shear wave) and at $\omega \gg \omega_1$ and $\mathbf{Y}_0 = 0$ with phase velocities C_l and $C_{s\alpha}$. This is a reasonable result: from the dispersion curves and the equation of motion we see that in these limits the medium behaves as a classical elastic medium with corresponding constants. One of the main differences with the classical elasticity is the strong frequency dependence in amplitude and wavenumber. Another one is the localization for a certain domain of frequencies: in the forbidden zone ($\omega_1 < \omega < \omega_0$) part of the source energy is stored near the source; we see that only the part associated with the *P*-wave propagates and the one associated with the shear waves exponentially decays.

These expressions are valid for $\omega \neq \omega_0$ and $\omega \neq \omega_1$. At $\omega = \omega_0$, if $\mathbf{Y}_0 \neq 0$, we have a resonance solution for $\boldsymbol{\theta}$. For $\mathbf{u}$ we have

$$\mathbf{u} = -\frac{\mathbf{X}_0 e^{i\omega_0 t}}{4\pi\rho\omega_0^2} \cdot \left\{ \frac{\tilde{e} - 3\hat{\mathbf{r}}\,\hat{\mathbf{r}}}{r^3} - e^{-i\frac{\omega_0}{C_l}r}\left[\frac{1}{r}\frac{\omega_0^2}{C_l^2}\hat{\mathbf{r}}\,\hat{\mathbf{r}} + \left(1 + i\frac{\omega_0}{C_l}r\right)\frac{\tilde{e} - \hat{\mathbf{r}}\,\hat{\mathbf{r}}}{r^3}\right]\right\} - \frac{\mathbf{Y}_0 e^{i\omega_0 t}}{8\pi\alpha^2} \cdot \frac{\tilde{e} \times \hat{\mathbf{r}}}{r^2}. \quad (11)$$

We observe localization (localized wave, decaying as $1/r^3$) even for $\mathbf{Y}_0 = 0$. In the latter case at $\omega = \omega_0$ we have $\boldsymbol{\theta} = e^{i\omega_0 t}\mathbf{X}_0 \times \hat{\mathbf{r}}/(8\pi\alpha r^2)$.

The case of $\omega = \omega_1$ has to be considered separately. Starting from (2), we obtain

$$\begin{aligned}
\mathbf{u} &= -\frac{1}{4\pi}\frac{\mathbf{X}_0 C_s^2}{\mu\omega_1^2} e^{i\omega_1(t - r/C_l)} \cdot \left[\frac{1}{r}\frac{\omega_1^2}{C_l^2}\hat{\mathbf{r}}\,\hat{\mathbf{r}} + \left(1 + i\frac{\omega_1}{C_l}\right)\frac{\tilde{e} - 3\hat{\mathbf{r}}\,\hat{\mathbf{r}}}{r^3}\right] - \frac{C_{S\alpha}^2}{2\alpha\omega_1^2}\ \mathrm{rot}\,\mathbf{Y}_0\delta(\mathbf{r})e^{i\omega_1 t}, \\
\boldsymbol{\theta} &= e^{i\omega_1 t}\frac{\mu + \alpha}{4\alpha^2}\left[\mathbf{Y}_0\delta(\mathbf{r}) + \frac{C_{S\alpha}^2}{\omega_1^2}\mathbf{Y}_0\triangle\delta(\mathbf{r}) - \frac{C_{S\alpha}^2}{\omega_1^2}\ \mathrm{grad\ div}\,\mathbf{Y}_0\delta(\mathbf{r})\right].
\end{aligned} \quad (12)$$

We see that a strong localization takes place at $\omega = \omega_1$ if the external torque $\mathbf{Y}_0 \neq 0$.

Solution for the Surface Rayleigh Wave

Consider the wave propagation along the surface of the free elastic half-space. Let z be the vertical coordinate with the corresponding unit vector $\mathbf{i}_3$, and x and y—coordinates in the plane (axes $\mathbf{i}_1$ and $\mathbf{i}_2$). We look for the solution of (1) in the form of

$$\begin{aligned}
u_j(x, z, t, k) &= \int_{-\infty}^{\infty} U_j(z) e^{i(kx + \omega t)}\hat{s}_0(\omega)\, d\omega, \\
\theta_j(x, z, t, k) &= \int_{-\infty}^{\infty} W_j(z) e^{i(kx + \omega t)}\hat{s}_0(\omega)\, d\omega,
\end{aligned} \quad (13)$$

where i is the imaginary unit, k is the wavenumber, ω is the circular frequency, t is the time, $U_j(z)$ and $W_j(z)$ are amplitude functions depending on depth, and $\hat{s}_0(\omega)$ is the complex spectral function corresponding to the Fourier spectrum of a source signal and determines the wavepacket form. The subscript j takes values x, y, and z.

The equation of motion (1) then separates in two independent systems of equations: one for $U_x(z)$, $U_z(z)$, and $\theta_y(z)$ and the other for $U_y(z)$, $\theta_x(z)$, and $\theta_z(z)$. To investigate the Rayleigh-type wave in the medium, we look for the solutions of the first system decreasing with depth z. We have

$$\begin{aligned}
&u_x(x, z, t) \\
&= \int_{-\infty}^{\infty} k\left(e^{-\nu_1 z} - \frac{2\nu_1\nu_2 C_s^2}{2k^2C_s^2 - \omega^2}e^{-\nu_2 z}\right)e^{i(kx + \omega t - \pi/2)}\hat{s}_0(\omega)\, d\omega, \\
&u_z(x, z, t) \\
&= \int_{-\infty}^{\infty} \nu_1\left(e^{-\nu_1 z} - \frac{2k^2C_s^2}{2k^2C_s^2 - \omega^2}e^{-\nu_2 z}\right)e^{i(kx + \omega t)}\hat{s}_0(\omega)\, d\omega, \\
&\theta_y(x, z, t) \\
&= \int_{-\infty}^{\infty} \frac{-\nu_1 k\omega^2}{(2k^2C_s^2 - \omega^2)(1 - \omega^2/\omega_1^2)}e^{-\nu_2 z}e^{i(kx + \omega t - \pi/2)}\hat{s}_0(\omega)\, d\omega.
\end{aligned} \quad (14)$$

Applying the boundary condition $\mathbf{i}_3 \cdot \tilde{\sigma} = 0$, we obtain the dispersion relation for the Rayleigh wave:

$$-4\nu_1\nu_2 k^2 + \left(2k^2 - \frac{\omega^2}{C_s^2}\right)^2 = 0, \quad \text{where } \nu_1 = \sqrt{k^2 - \frac{\omega^2}{C_l^2}}, \quad \nu_2 = \sqrt{k^2 - \frac{\omega^2}{C_s^2}\left(\frac{1 - \omega^2/\omega_0^2}{1 - \omega^2/\omega_1^2}\right)}. \quad (15)$$

The denominator of ν_2 equals zero at the critical frequency $\omega = \omega_1$. The surface wave will exist only provided that $\nu_m \in \mathbb{R}$, $\nu_m > 0$, and $m = 1, 2$.

Curves $\nu_1 = 0$ and $\nu_2 = 0$, bounding the allowed zone for the Rayleigh wave, are the dispersion relations for the compression and shear-rotation plane waves in 3D, respectively. The allowed zone is shown in Figure 2. We have proved the following features of equation (15):

1. The Rayleigh wave at high frequencies is slower than both the shear-rotation wave at high frequencies and the compression wave in the 3D unbounded medium: $C_\infty < C_{s\alpha}$ and $C_\infty < C_l$. At these high frequencies, the rotational degrees of freedom are almost embedded into the background continuum, and the medium behaves as the classical medium with 3D phase velocities C_l and $C_{s\alpha}$.

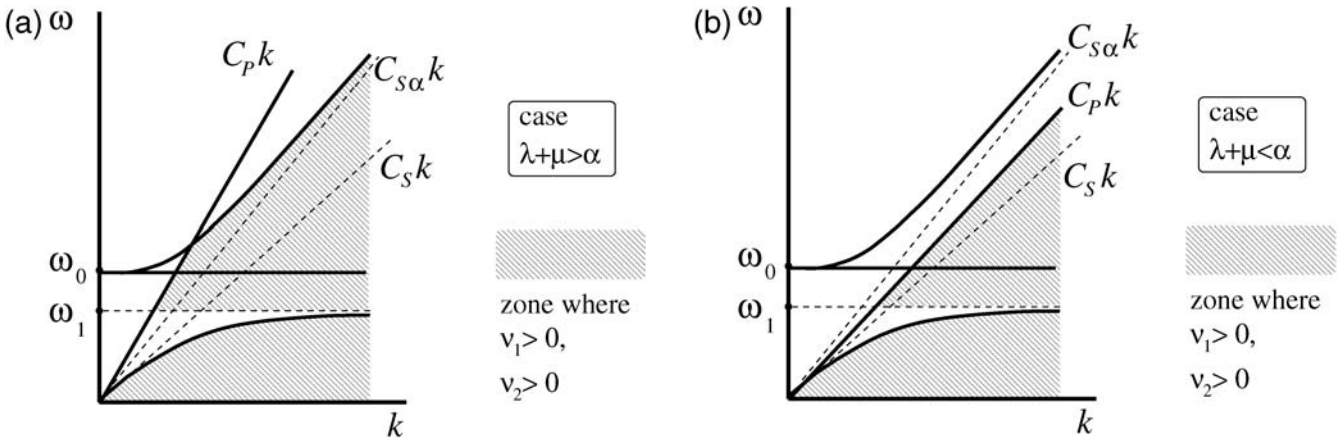

Figure 2. Allowed zones for Rayleigh waves.

2. At the same time, the Rayleigh wave at high frequencies can be faster than the shear wave in the unbounded 3D medium at small frequencies: $C_\infty > C_s$.
3. At $\omega \to 0$ the velocity of the Rayleigh wave tends to the velocity of the Rayleigh wave in the classical medium with Lamé constants λ and μ and, consequently, is less than the plane shear-wave velocity in this medium.
4. At $\omega \to \omega_1 - 0$ the dispersion equation (15) has no solution. Thus there is a forbidden band of frequencies lying below ω_1, where the Rayleigh-type wave does not exist. Apparently, in this band of frequencies the perturbations stay localized near the source, and the rotational degrees of freedom trap the wave energy.
5. There is a solution: $k \to \infty$, $\omega = O(1)$, corresponding to the case of an infinitely large wavenumber for a certain critical frequency $\omega_2 = \omega_1 \sqrt{A/(1+A)} < \omega_1$, where $A = (1 + \mu/\alpha)[1 - \mu/(\lambda + 2\mu)]$. One of dispersion curves has an asymptote $\omega = \omega_2$. At $\omega = \omega_2$ and at $\omega \to \omega_2 + 0$ the Rayleigh wave does not exist, for example, there is a forbidden band of frequencies above ω_2.

In all numerical examples we have seen that the whole band of frequencies $(\omega_2; \omega_1)$ is forbidden, but we have not proved theoretically that this is always so. The numerical analysis of the dispersion relation (15) for the constants $\lambda = 28 \times 10^9$, $\mu = 4 \times 10^9$, $\alpha = 2 \times 10^9$, and $I = 10^3$ (in the International System of Units) is represented in Figure 3. The solid line corresponds to the reduced Cosserat continuum, and the dashed horizontal line corresponds to the Rayleigh-wave velocity in a classical medium. The vertical lines bound the frequency interval $(\omega_2; \omega_1)$. In this frequency range the Rayleigh wave cannot propagate; it may mean that localization phenomena are possible for these frequencies. Apart from that, near this domain we observe dispersive behavior. At very low and very high frequencies, at least for the given parameters, the behavior is close to the classical one (but with different elastic constants).

Conclusions

The rotational dynamics of heterogeneities in rocks and soils, taken into account by means of the reduced Cosserat continuum model, gives a strong frequency dependence both for the plane shear-rotation waves and the waves induced by a harmonic point source in 3D unbounded medium, as well as for the Rayleigh-type wave. We have more dispersion branches than in the classical case and a different type of polarization. There are forbidden bands of frequencies, where the energy of the wave is trapped by the rotational dynamics

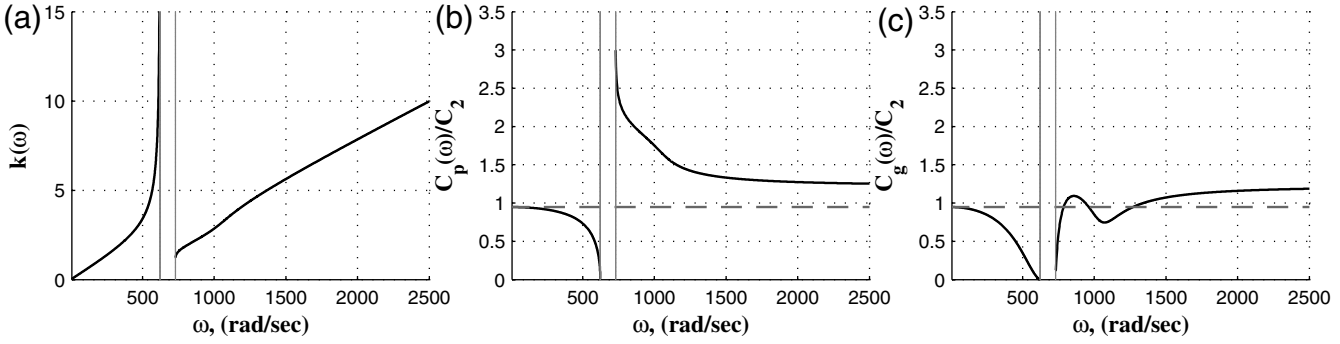

Figure 3. Numerical example illustrating the behavior of (a) wavenumber, (b) phase, and (c) group velocities for a Rayleigh wave in the reduced Cosserat continuum.

of the microstructure, that is, the corresponding waves (or a part of the wave in the case of dynamic point sources) do not propagate, and localization near the source is possible.

The forbidden band for the Rayleigh wave lies precisely below the forbidden band for the 3D case. Near these forbidden bands we observe strong dispersion. There is a frequency where we observe resonantlike behavior for the rotational displacement in the presence of external torque load. This can be seen in the expression for the Green's functions. For the Rayleigh wave we have, apart from the boundary and cutoff frequencies, also a cutoff wavenumber, where one of the dispersion branches starts. The wave behavior differs from the classical case as well as from the full Cosserat continuum with nonzero couple stresses, where we have no forbidden frequency bands and polarization is different.

The predicted effects are comparable to the ones observed in scattering by wavelength-sized objects in an elastic medium. This indicates that our model could eventually represent an effective medium that accounts for the frequency-dependent transmission of shear waves.

In both—reduced and full—Cosserat models, in contrast to the classical elasticity, the dispersion of the Rayleigh wave and of bulk plane shear-rotation waves is present. The main difference between the full and reduced Cosserat models is the presence of a forbidden zone of frequencies in the reduced model, where the Rayleigh and shear-rotation waves do not propagate, and the absence of such a zone in the full Cosserat model.

The results obtained in this article can be used for the preparation and interpretation of seismic experiments, which could validate the importance of asymmetric theories of elasticity in earthquake and exploration seismology, and for experimental determination of the material constants of the Cosserat media.

Data and Resources

No data were used in this article. Some plots were made using the Matlab (http://www.mathworks.com/products/matlab/, last accessed June 2008).

Acknowledgments

This work was supported by the U.S. Civilian Research & Development Foundation (Post-Doctoral Fellowship Program Y2-P-09-04), by Shell International E.& P., by the Government of Andalucía (Project Number FQM-421), and by the Spanish government (Project Number FIS2006-03645).

References

Cosserat, E., and F. Cosserat (1909). *Theórie des Corps Déformables*, Hermann, Paris.

Eringen, A. C. (1998). *Microcontinuum Field Theories. I. Foundation and Solids*, Springer-Verlag, New York.

Hudson, J. A., and L. Knopoff (1989). Predicting the overall properties of composite materials with small-scale inclusions or cracks, *Pure Appl. Geophys.* **131,** no. 4, 551–576.

Kafadar, C. B., and A. C. Eringen (1971). Micropolar media, *Int. J. Eng. Sci.* **9,** 271–305.

Kulesh, M. (2009). Waves in linear elastic media with microrotations, part 1: Isotropic full Cosserat model, *Bull. Seismol. Soc. Am.* **99,** no. 2B, 1416–1422.

Miklowitz, J. (1978). *Elastic Waves and Waveguides*, North-Holland, Amsterdam.

Nowacki, W. (1986). *Theory of Asymmetric Elasticity*, Pergamon Press, Oxford, U.K.

Okada, Y. (1985). Surface deformation due to shear and tensile faults in a half-space, *Bull. Seismol. Soc. Am.* **75,** no. 4, 1135–1154.

Schwartz, L. M., D. L. Johnson, and S. Feng (1984). Vibrational modes in granular materials, *Phys. Rev. Lett.* **52,** no. 10, 831–834.

Suiker, A. S. J., R. de Borst, and C. S. Chang (2001). Micro-mechanical modelling of granular material. Part I: Derivation of a second-gradient micro-polar constitutive theory, *Acta Mechanica* **149,** no. 1, 161–180.

Vardoulakis, I. (1989). Shear-banding and liquefaction in granular materials on the basis of a Cosserat continuum theory, *Arch. Appl. Mech. (Ingenieur Archiv)* **59,** no. 2, 106–113.

Institute for Problems in Mechanical Engineering RAS
Bolshoy pr, V.O., 61
St. Petersburg, 199178, Russia
elgreco@pdmi.ras.ru
(E.F.G.)

Institute of Continuous Media Mechanics
Ural Division
Russian Academy of Sciences
Perm 614013, Russia
kma@icmm.ru
(M.A.K.)

Shell International E. & P.
Kessler Park 1, 2288 GS
Rijswijk, The Netherlands
(G.C.H.)

Manuscript received 25 June 2008